3de Belgisch Nationaal Congres over Theoretische en Toegepaste Mechanica

3ème Congrès National Belge de Mécanique Théorique et Appliquée

Université de Liège - Campus du Sart Tilman

30 - 31 mei 1994
30 - 31 mai 1994

Organisé par le
Georganiseerd door het

Comité National de Mécanique Théorique et Appliquée

Nationaal Comité voor Theoretische en Toegepaste Mechanica

REFERAAT
ACTES

Uitgevers / Editeurs :
M. HOGGE (ULG) / E. DICK (UG)

OVERHEAD TRANSMISSION LINE GALLOPING
A COMPARATIVE STUDY BETWEEN 2-DOF AND 3-DOF MODELS

J. Wang and J.L. Lilien
Université de Liège, Institut d'Electricité Montefiore
Sart-Tilman B.28, B-4000 Liège

Abstract- A three-degree-of-freedom (3-DOF) iced-conductors model for galloping analysis, including second order coupling terms and for both single and bundle conductors, is described. The comparison between 2-DOF and 3-DOF models, and some applications with the new model are detailed.

1. Introduction

The phenomena of galloping is a large amplitude, low frequency and wind-induced oscillation of overhead transmission lines. Galloping mechanism is very closely related to the couplings between horizontal, vertical and torsional movement. Galloping used to be studied in a 2-DOF system (vertical and torsion), even in 3-DOF system (horizontal in addition), the existing theories usually neglected some second order couplings and were only sufficient to explain the galloping of single conductor, not that of bundle ones[6,7,8]. This paper describes an approach in a 3-DOF system including bundle conductors, some improvements on the currently used model and a comparative study between 2-DOF and 3-DOF models.

2. Mathematical formulation

Basic Hypothesis

Due to the fact that the galloping frequency is very low, it is enough to consider only the first three eigen modes for modal decomposition. The rotation is around the centre of the cable for single conductor and the centre position for bundle one whatever this position is. Subconductors are uniformly distributed along the circumferential geometry and subspans are identical along one span. Spacer arms are rigidly connected so that the angle θ for bundle is the rotation angle of the spacers.

The 3-DOF Conductor System

The basic second-order partial derivatives equations for vertical, torsional and horizontal motion can be found in the literature for cable structures [1].

From basic expressions of conductor's motion and based on a 2-DOF system [1,2], Modal decomposition is used with the function

$$f(z,t) = \sum_{k=1}^{\infty} f_k(t) \sin k\delta \quad with \quad \delta = \frac{\pi z}{L} \qquad (1)$$

where f represents vertical displacement y, horizontal one x and the torsional angle θ, respectively. t is time, L and z are span length and the distance from the beginning anchoring of the line section to the point where to be studied. k is modal number.

The 3-DOF conductor system with each mode k is described by

$$m\ddot{y}_k + C_y\dot{y}_k + T(\tfrac{k\pi}{L})^2 y_k = \tfrac{2}{\pi}\textstyle\int_0^{\pi}[-mg + f_v]\sin k\delta d\delta \qquad (2)$$

$$I\ddot{\theta}_k + C_\theta\dot{\theta}_k + GJ\theta_k = \frac{2}{\pi}\int_0^{\pi}[M_w]\sin k\delta d\delta \qquad (3)$$

$$m\ddot{x}_k + C_x\dot{x}_k + T(\frac{k\pi}{L})^2 x_k = \frac{2}{\pi}\int_0^{\pi}[f_h]\sin k\delta d\delta \qquad (4)$$

where the coefficient C_y, C_θ and C_x represent the damping in 3-DOF. T and GJ are the tension and torsional stiffness. The f_v,M_w and f_h are corresponding the external excitations on the conductor system. They are combined by the aerodynamic drag, lift and moment due to the dissymmetrical profile, which are given in appendix. Furthermore, m and I are the mass and the moment of inertia of the iced conductor's cross section. The definition for angles and forces is shown in figure 1.

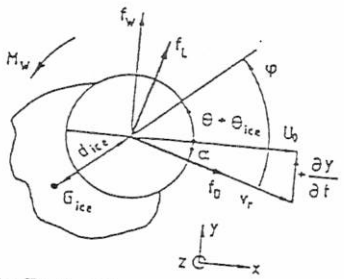

Figure 1: Definition for angles and forces

The source of the external excitations is *wind*. The wind velocity relative to the conductor is described by

$$V_r = \{[V_{0x} - R\dot{\theta}\sin(\theta_0+\theta) - \dot{x}]^2 + [V_{0y} + R\dot{\theta}\cos(\theta_0+\theta) - \dot{y}]^2\}^{\frac{1}{2}} \qquad (5)$$

where θ_0 is the angle in the original equilibrium position, generally it is the ice accretion angle θ_{ice}. V_{0x} and V_{0y} are the components of the true wind velocity V_0. R is the radius of subconductor.

In the galloping system, one of the most active factors is *angle of attack* . It is defined by

$$\varphi = \theta_0 + \theta - \frac{r_i}{V_0}\dot{\theta} - \alpha \tag{6}$$

where $r_i = d_{ice}$, is the distance between the center of conductor and the center of the ice gravity.

The angle α is given by

$$\alpha = \frac{V_{0y} + R\dot{\theta}\cos(\theta_0+\theta) - \dot{y}}{V_{0x} - R\dot{\theta}\sin(\theta_0+\theta) - \dot{x}} \tag{7}$$

For the purpose of stability analysis, the system needs to be linearized. Under the basic approximation and affter the linearization, the linearized external aerodynamic excitations on the conductor system are described by

$$\begin{aligned}\Delta f_v = K_D V_0 &((C_{L\alpha} - C_D)\Delta\dot{y} \\ &+C_{L\alpha}V_0\Delta\theta - C_{L\alpha}r_i\Delta\dot{\theta} - 2C_L\Delta\dot{x})\end{aligned} \tag{8}$$

$$\begin{aligned}\Delta f_h = K_D V_0 &((C_{D\alpha} + C_L)\Delta\dot{y} \\ &+C_{D\alpha}V_0\Delta\theta - C_{D\alpha}r_i\Delta\dot{\theta} - 2C_D\Delta\dot{x})\end{aligned} \tag{9}$$

$$\begin{aligned}\Delta M_w = K_M V_0 &(C_{M\alpha}\Delta\dot{y} + C_{M\alpha}V_0\Delta\theta \\ &-C_{M\alpha}V_0 r_i\Delta\dot{\theta} - 2C_M\Delta\dot{x})\end{aligned} \tag{10}$$

where C_D, C_L and C_M are aerodynamic coefficients of drag, lift and moment. $C_{D\alpha}$, $C_{L\alpha}$ and $C_{M\alpha}$ are their first order derivatives to φ respectively. K_D and K_M are defined in appendix.

Therefore, the linearized conductor system in 3-DOF, including the second order coupling terms between vertical, horizontal and torsional modes, is obtained by:

$$\begin{aligned}&\Delta\ddot{y}_k + \left(\tfrac{C_y}{m} + \tfrac{K_D V_0}{m}\left(\overline{C}_{L\alpha} - \overline{C}_D\right)\right)\Delta\dot{y}_k \\ &+\omega_{v,k}^2\Delta y_k \\ &= \tfrac{K_D V_0^2}{m}\overline{C}_{L\alpha}\Delta\theta_k - \tfrac{K_D r_i V_0}{m}\overline{C}_{L\alpha}\Delta\dot{\theta}_k \\ &\quad - \tfrac{m_i r_i}{m}\overline{\sin\theta_0}\Delta\ddot{\theta}_k - \tfrac{2K_D V_0}{m}\overline{C}_L\Delta\dot{x}_k\end{aligned} \tag{11}$$

$$\begin{aligned}&\Delta\ddot{x}_k + \left(\tfrac{C_x}{m} + \tfrac{2K_D V_0}{m}\overline{C}_D\right)\Delta\dot{x} + \omega_{v,h}^2\Delta x_k \\ &= \tfrac{K_D V_0}{m}\left(\overline{C}_{D\alpha} + \overline{C}_L\right)\Delta\dot{y}_k + \tfrac{K_D V_0^2}{m}\overline{C}_{D\alpha}\Delta\theta_k \\ &\quad - \tfrac{K_D r_i V_0}{m}\overline{C}_{D\alpha}\Delta\dot{\theta}_k - \tfrac{m_i r_i}{m}\overline{\cos\theta_0}\Delta\ddot{\theta}_k\end{aligned} \tag{12}$$

$$\begin{aligned}&\Delta\ddot{\theta}_k + \left(\tfrac{C_\theta}{I} + \tfrac{K_M r_i V_0}{I}\overline{C}_{M\alpha}\right)\Delta\dot{\theta}_k \\ &+\left(\tfrac{GJ}{I}\left(\tfrac{k\pi}{L}\right)^2 - \tfrac{K_M V_0^2}{I}\overline{C}_{M\alpha} + \tfrac{m_i g r_i}{I}\overline{\sin\theta_0}\right)\Delta\theta_k \\ &= \tfrac{K_M V_0}{I}\overline{C}_{M\alpha}\Delta\dot{y}_k + \tfrac{m_i r_i}{I}\overline{\cos\theta_0}\Delta\ddot{y}_k \\ &\quad - \tfrac{2K_M V_0}{I}\overline{C}_M\Delta\dot{x}_k + \tfrac{m_i r_i}{I}\overline{\sin\theta_0}\Delta\ddot{x}_k\end{aligned} \tag{13}$$

The modified aerodynamic coefficients are given by

$$\overline{\Psi} = \frac{2}{\pi}\int_0^\pi \Psi\sin^2 k\delta d\delta \tag{14}$$

where Ψ represents C_D, C_L, C_M, $C_{D\alpha}$, $C_{L\alpha}$, $C_{M\alpha}$, $\sin\theta_0$ and $\cos\theta_0$, respectively.

From these linearized conductor system equations, it is clearly to see the coupling terms and the aerodynamic dampings.

3. Approach on tension

For a N-span section with any configuration, we have [1]:

$$\Delta T = K_e\Delta l \tag{15}$$

where

$$\frac{1}{K_e} = \frac{\sum_{j=1}^N L_j}{EA} + \frac{1}{K_1} + \frac{1}{K_2} \tag{16}$$

K_e is the equivalent stiffness, K_1 and K_2 represent the anchoring stiffness of two end towers. E and A are Young modulus and the conductor cross section of one phase.

The length variation of the span in 3-DOF can be expressed by

$$\Delta l \simeq \frac{1}{2}\int_0^L \{[(\frac{dy}{dz})^2 - (\frac{dy_0}{dz})^2] + [(\frac{dx}{dz})^2 - (\frac{dx_0}{dz})^2]\}dz \tag{17}$$

and the global length variation of the section is given by

$$\Delta l_g = \sum_{j=1}^N L_j\sum_{k=1}^3 (\frac{k\pi}{2L_j})^2[(y_{j,k}^2 - y_{j,k0}^2) + (x_{j,k}^2 - x_{j,k0}^2)] \tag{18}$$

Therefore, the global tension of cable is obtained by

$$T = T_0 + K_e\Delta l_g \tag{19}$$

The Movement of Insulator

Because suspension insulator motions in both horizontal and vertical have nearly no influence for the cable length in a N-span section. By considering its longitudinal movement Δz_j in figure 2, the deformed length of j^{th} span is obtained by

$$l_j = L_j + \Delta l_g + \Delta z_j - \Delta z_{j-1} \tag{20}$$

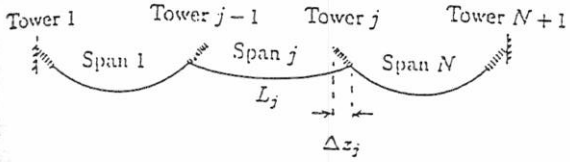

Figure 2: Definition for insulator movement

where Δz_j is given by

$$\Delta z_j = \frac{(T_j - T_{j-1}) l_{ins}}{\sqrt{\begin{array}{c}(T_{j-1}\tan\varphi_{j-1} - T_j \tan\varphi_j \\ + \frac{M_{insg}}{2})^2 + (T_j - T_{j-1})^2\end{array}}} \quad (21)$$

The tension is transformed by the movement of insulators. This is the main reason that tension can get good compensation sometimes and it nearly has the same value along a subconductor. But between subconductors, the tension is different due to the torsion (see part 5).

Tension in Bundle Conductor

At any point P along subconductor i, the tension distribution in both x and y are given by

$$\begin{pmatrix} T_x \\ T_y \end{pmatrix} = T_i \begin{pmatrix} \frac{\partial x_i}{\partial z} \\ \\ \frac{\partial y_i}{\partial z} \end{pmatrix} \quad (22)$$

$$T_i = \frac{T_0}{n} + \Delta T_i \quad (23)$$

$$\Delta T_i = [\frac{nL}{EA}\mathrm{U} + 2\mathrm{F}]^{-1}_{i;i} \Delta l_i \quad (24)$$

where F is the flexibility matrix [3].

If we analyze the bundle around the static equilibrium position (y_t, x_t, θ_t), the variation expression of length can be obtained by

$$\Delta l_i = (r \int_0^L \Delta\theta dz)\left(\frac{\partial^2 x_t}{\partial z^2}\sin\sigma - \frac{\partial^2 y_t}{\partial z^2}\cos\sigma\right) \quad (25)$$

where r is a half of the spacing. σ is the angular position of subconductor, refer to horizontal. By this way, tension variations between subconductors can be obtained. It must be pointed out that, in spite of their weakness, the tension variations between subconductors may increase the bundle stiffness more than 50%.

An Example on Tension Distribution

By applying a static torque at the mid-span of one span in the section, the variations of subconductor length and subconductor tension, as well as distributed forces on spacers due to the tension variations can be obtained.

Case 1: AMS $2 \times 620mm^2$, Horizontal Bundle, deadend span section. subconductor cross section $A = 620mm^2$, Young modulus $E = 5.3 \times 10^{10} N/m^2$, mass of subconductor $m = 1.8kg/m$, subconductor diameter $\phi = 32.4mm$, subconductor separation $d = 0.45m$, sagging tension per subconductor $T = 31000N$, intrinsic torsional stiffness $\tau = 460Nm^2$, span length $L = 483.2m$, with 6 spacers and a $60Nm$ static torque at the mid-span.

The distributed forces due to the tension can be simulated. It is shown in table 1.

Obviously, the tension is mainly distributed in vertical.

4. Effects of horizontal movement

As a degree of freedom, horizontal movement has effects coupled with others. The example to show the effects of horizontal movement are simulated as following:

Case 2: the basic data are same as case 1, but with a $275.5Nm^2$ intrinsic torsional stiffness and with a 45 degrees ice accretion angle θ_{ice}.

The values in equilibrium position are shown in table 2 and table 3:

V_0 (m/s)	T (N)	y (m)	$\theta(deg.)$
5	66233.6	16.02	46.80
10	69975.8	16.17	50.67
15	75178.4	16.36	56.46

Table 2: Without horizontal movement

V_0 (m/s)	T (N)	y (m)	x (m)	$\theta(deg.)$
5	66313.5	16.00	0.89	46.76
10	71304.6	15.86	3.40	50.58
15	81350.0	15.10	6.95	56.58

Table 3: With horizontal movement

From this example, we can find the tension in 2-DOF is obviously lower than that in 3-DOF with the same wind speed, and the tendency of vertical displacement in these two kinds DOF are opposite when the wind speed is getting strong. The influences of horizontal motion have obvious effects on torsional motion, but it also depends on the ice accretion angle. Moreover, for a horizontal twin bundle with zero ice accretion, the increasing of horizontal movement also makes the torsional stiffness increased.

5. Applications

Stiffness Matrix for Stability Analysis

From Eq.(19), the tension variation for stability analysis with a N-span section around the equilibrium position is obtained by

spacer No.	1	2	3	4	5	6
x force(N)	0.18	-0.63	-15.27	-15.27	-0.63	0.18
y force(N)	1079.05	1397.32	1191.05	1191.05	1397.32	1079.05

Table 1: Distributed forces on spacers

torque(Nm)	finite element results[4]		3-DOF model results	
	$\theta_{\frac{L}{2}}$(deg.)	ΔT_1,ΔT_2(N)	$\theta_{\frac{L}{2}}$(deg.)	ΔT_1,ΔT_2(N)
26.4	15.54	-398, 399	15.51	-403.9, 403.9
67	42.9	-1042, 1050	42.6	-1061, 1061
98.13	77.6	-1613, 1672	74.73	-1668, 1668
100.8	83.75	-1698, 1751	79.23	-1732, 1732

Table 4: Rotation angles and tension variations

$$\Delta T = \frac{K_e}{2m}\sum_{j=1}^{N} L_j \sum_{k=1}^{3}(\frac{k\pi}{L_j})^2 y_{j,k0}\Delta y_{j,k} + \frac{K_e}{2m}\sum_{j=1}^{N} L_j \sum_{k=1}^{3}(\frac{k\pi}{L_j})^2 x_{j,k0}\Delta x_{j,k} \quad (26)$$

Furthermore, we can get the stiffness matrix for one span:

$$\begin{pmatrix} \omega_v^2 + K_{yy} & 0 & K_{yx} \\ 0 & \omega_\theta^2 & 0 \\ K_{xy} & 0 & \omega_h^2 + K_{xx} \end{pmatrix} \quad (27)$$

with

$$K_{yy} = \frac{K_e}{2m}\sum_{k=1}^{3}\frac{(k\pi)^4}{L^3}y_{k0}^2$$

$$K_{xx} = \frac{K_e}{2m}\sum_{k=1}^{3}\frac{(k\pi)^4}{L^3}x_{k0}^2$$

$$K_{xy} = K_{yx} = \frac{K_e}{2m}\sum_{k=1}^{3}\frac{(k\pi)^4}{L^3}y_{k0}x_{k0}$$

A Comparison with Finite Element Results

Case 3: ACSR $2 \times 470mm^2$, Horizontal Bundle, 2-span section. subconductor cross section $A = 470mm^2$, Young modulus $E = 7.5\times10^{10}N/m^2$, mass of subconductor $m = 1.28kg/m$, subconductor diameter $\phi = 28.2mm$, subconductor separation $d = 0.457m$, sagging tension per subconductor $T = 35600N$, span length $L_1 = L_2 = 244m$, with 3 spacers, The result is shown in table 4.

This comparison shows very closed results, not only for small rotation, but also for large rotation.

6. Conclusions

This 3-DOF system model takes into account the coupling factors as fully as possible and includes the second order coupling terms between vertical, horizontal and torsional modes. It has been proved in this paper that a simple 3-DOF model fully agrees with the complex finite element software for the close relationship between all the DOF and the tension in the cable. This model can be then used for the modelization of galloping by simple approach. The effects of tension oscillation during the galloping and its influence on torsional stiffness will be valid for simulation. The 3-DOF model is much more valid than 2-DOF one, especially for equilibrium positions.

Appendix

The aerodynamic drag, lift and moment:

$$f_D = K_D V_r^2 C_D(\varphi)$$

$$f_L = K_D V_r^2 C_L(\varphi)$$

$$M_w = K_M V_r^2 C_M(\varphi)$$

with $K_D = \frac{1}{2}\rho_{air}\phi$ and $K_M = \frac{1}{2}\rho_{air}\phi^2$.

References

1. J.L.Lilien, H.Dubois and F.Dal Maso. AIM study day on Galloping,Liège,pp5.1-5.42,march 1989.

2. J.L.Lilien, H.Dubois. Proceedings,IEE Overhead line design and construction,Nov.1988,pp65-69.

3. H.Dubois, J.L.Lilien and F.Dal Maso. Rev. AIM-Liège $n^0$1/1991,pp45-62.

4. Samcef-Cable. SAMTECH S.A.,Bd Frère ORBAN 25,4000 Liège.

5. H.Max Irvine. Cable Structures,MIT Press,19

6. R.D.Blevins, W.D.Iwan. Journal of Applied Mechanics,Dec.1974,pp1113-1118.

7. O.Nigol, P.G.Buchan. IEEE Trans.PAS, Vol.100,No.2,Feb.1981,pp708-720.

8. P.Yu, A.H.Shah, N.Popplewell. Trans. ASME,March 1992,Vol.59,pp140-145.